Morphological Origin of the Multistep Relaxation Behavior in Semicrystalline Ethylene/Methacrylic Acid Ionomers

Katsuyuki Wakabayashi and Richard A. Register*

Department of Chemical Engineering, Princeton University, Princeton, New Jersey 08544-5263

Received September 25, 2004; Revised Manuscript Received November 29, 2005

ABSTRACT: Ethylene/methacrylic acid (E/MAA) ionomers contain polyethylene crystallites, amorphous polymer segments, and ionic aggregates. While the property changes observed upon neutralization of the MAA units are often attributed to the formation of ionic aggregates, no quantitative description currently exists for how these three structural motifs—alone or in combination—control any of these material properties. In this paper, we define such relationships for perhaps the most basic mechanical property of interest: the small-strain modulus. At temperatures just below the melting point of the primary crystallites, the ionomers can be satisfactorily described as two-phase composites of crystallites and ionically cross-linked rubber; however, at room temperature, the modulus is far higher than such a description predicts. We trace this effect to a synergy between the ionic aggregates and secondary crystallites, which together form percolated rigid pathways through the amorphous phase at room temperature. When the secondary crystallites melt, these paths break down and the simple two-phase composite description is recovered.

Introduction

Ionomers are thermoplastics that contain a small fraction of ionic functional groups pendant to the polymer backbone.[1−3] A well-known and much-studied class of ionomers encompasses those derived from semicrystalline ethylene−methacrylic acid and ethylene−acrylic acid (E/(M)AA) copolymers, by partially or fully neutralizing with a metal cation such as sodium, magnesium, or zinc.[4] Neutralization ("ionomerization") and consequent aggregation of these ionic groups produces marked differences in optical, mechanical, and other physical properties when compared with E/(M)AA copolymers or low-density polyethylenes.[4] These ionic aggregates are contained within the amorphous regions between polyethylene-like crystallites,[5−7] producing a rich nanostructured morphology. While the property changes which accompany ionomerization must ultimately derive from this morphology, it is unclear how these various structural motifs, alone or in combination, dictate the material properties of such semicrystalline ionomers.

Even in the absence of crystallinity, the mechanical response of ionomers can be complex. Dynamic mechanical thermal analysis (DMTA) on amorphous styrene/MAA,[8−10] styrene/AA,[9] and vinylcyclohexane/AA[9] ionomers revealed two distinct relaxations, which Eisenberg, Hird, and Moore (EHM)[11] interpreted as the glass transitions of two different phases. The lower-temperature relaxation, which occurs at a temperature only modestly above that of the nonionic homopolymer, was attributed to the glass transition of the ion-depleted matrix, while the higher-temperature relaxation was associated with devitrification of the ionic aggregates and neighboring polymer segments, within what EHM termed a "region of restricted mobility". Though the volume fraction of ionic units is typically small in ionomers, the small size of the ionic aggregates—especially when the ionic group is close to the polymer backbone, as in MAA and AA salts[9,12,13]—and their immobilization of an adjacent layer of polymer can make the higher-temperature relaxation of these ion-rich regions the dominant process at sufficiently high ion contents.[8,10,11]

* To whom correspondence should be addressed. E-mail: register@princeton.edu.

Dynamic mechanical studies conducted on semicrystalline E/MAA[14−16] and E/AA[17,18] ionomers also revealed two mechanical relaxations below the primary crystal melting temperature, suggesting that the amorphous regions in semicrystalline ionomers may have a morphology and dual-relaxation behavior similar to that in wholly amorphous ionomers. However, E/(M)AA ionomers possess a broad distribution of crystal thicknesses (resulting from the statistical nature of the acid incorporation), and the smaller secondary crystals can have thicknesses comparable to the distance between ionic aggregates.[19] Moreover, melting of the crystals (either primary or secondary) may overlap in temperature with the postulated devitrification of the ion-rich regions of the amorphous phase, leading to a complex relaxation and modulus-temperature behavior which has been difficult to interpret.

The aim of the present paper is to identify, separate, and quantify these different relaxation processes in typical semicrystalline E/MAA ionomers. We find that the stiffness increases which accompany ionomerization result from the formation of a sample-spanning "hard" phase at low ion contents. This percolated hard structure includes both crystallites and ion-rich amorphous regions, and its continuity can be tuned through sample thermal history to produce much larger variations in stiffness than are achievable in either amorphous ionomers or nonionic ethylene copolymers.

Experimental Section

Materials. E/MAA statistical copolymers containing 11.5, 15, 19, 22, and 28 wt % MAA (corresponding to ethylene mole fractions of 0.959, 0.946, 0.929, 0.916, and 0.888) served as the parent copolymers for the ionomers studied herein. These copolymers were synthesized via high-pressure free-radical copolymerization by DuPont Packaging and Industrial Polymers, and the acid contents were determined by titration. Table 1 lists all copolymers and ionomers used in this study, several of which have been employed in previous investigations from our group.[20−22] The sample code (e.g., 15−51Na) indicates the MAA content in the copolymer (15 = 15 wt % MAA) and the neutralization level (51Na = 51% of the MAA units neutralized with Na^+); unneutralized copolymers are labeled as 0Na. All E/MAA copolymers and ionomers with the exception of certain members of the 11.5 series

10.1021/ma052081v CCC: $33.50
Published on Web 01/05/2006

Table 1. Compositions and Selected Properties of E/MAA Ionomers Studied

ionomer	wt % Na	peak T_{m1}, °C	peak T_{m2}, °C	peak E'', °C	volume fraction crystallinity ϕ_1 (25 °C)	Young's modulus E (25 °C), MPa
11.5-0Na	0	96	39	2	0.26	100
11.5-7Na	0.22	96	39	4	0.26	140
11.5-10Na	0.31	97	40	5	0.27	200
11.5-16Na	0.49	96	41	18	0.26	250
11.5-26Na	0.79	96	43	25	0.26	250
11.5-39Na	1.20	96	46	32	0.23	290
11.5-47Na	1.44	96	46	37	0.24	300
11.5-62Na	1.89	95	47	38	0.22	300
11.5-83Na	2.51	93	49	41	0.19	280
15-0Na	0	91	39	10	0.21	120
15-24Na	0.96	92	46	32	0.20	420
15-34Na	1.36	91	47	36	0.19	400
15-51Na	2.03	90	48	40	0.16	410
15-67Na	2.64	89	48	41	0.14	390
19-0Na	0	90	40	16	0.19	190
19-8Na	0.41	89	44	29	0.21	460
19-14Na	0.71	89	45	32	0.19	530
19-22Na	1.12	88	46	37	0.16	520
19-35Na	1.77	87	46	39	0.14	500
19-51Na	2.55	86	48	44	0.14	480
22-0Na	0	86	40	25	0.16	360
22-26Na	1.52	86	45	41	0.13	580
22-35Na	2.04	84	46	41	0.11	540
22-48Na	2.77	85	47	41	0.08	540
28-0Na	0	79	42	33	0.10	630
28-12Na	0.90	77	43	41	0.07	810
28-19Na	1.42	78	45	42	0.06	810
28-28Na	2.07	78	45	44	0.08	800

were prepared by melt neutralization at DuPont; the neutralization level was determined by X-ray fluorescence. Ionomers 11.5-7Na, -10Na, -16Na, -26Na, and -47Na were prepared at Princeton via a solution process described previously;[20] melt rheological measurements show no difference between melt- and solution-neutralized ionomers.[20] Materials were melt-pressed at 130−140 °C into 0.2−0.4 mm thick sheets using a PHI hydraulic press, quenched to room temperature, and stored under vacuum or in a desiccator over $CaSO_4$ for 6 days unless otherwise specified. Specimens for different tests were taken from the same molded sheet to ensure identical thermal histories: ASTM D1708 dogbones were stamped out for uniaxial tensile testing, 5 × 30 mm rectangular strips were cut with a razor blade for DMTA, 7 × 31 mm strips were cut and stacked to ≈1 mm thickness for small-angle X-ray scattering (SAXS), and 7−10 mg specimens were punched from the sheets and encapsulated in aluminum volatile sample pans for differential scanning calorimetry (DSC).

Measurements. Uniaxial tensile testing was conducted at a constant crosshead speed of 2 in/min (initial strain rate of 0.038 s^{-1}) on an Instron 1122, equipped with a modified Environmental Chamber 3111 capable of temperature control within 0.3 °C. DMTA was conducted on a TA Instruments RSA 3, using the film fixture, at 1 Hz unless otherwise stated. The initial (low-temperature) strain amplitude was set at 0.1%, with auto-strain adjustments to allow for a maximum of 2% strain. Data were acquired at 4 °C intervals, for an average heating rate of 5 °C/min. DSC measurements were run at 5 °C/min on a Perkin-Elmer DSC-7 with type I intracooler, calibrated with indium and tin. SAXS patterns were collected using Cu Kα X-rays (wavelength $\lambda = 0.154\ 18$ nm) from a sealed tube source, an evacuated compact Kratky camera (Anton Paar), and an MBraun OED-50M one-dimensional position-sensitive detector. Detailed information on the SAXS system, as well as the data reduction procedure, may be found elsewhere;[23] SAXS patterns are presented as desmeared absolute intensity I/I_eV vs the magnitude of the momentum transfer vector $q = (4\pi/\lambda) \sin \theta$, where θ is half the scattering angle.

Results and Discussion

Modulus of the Amorphous Phase and Its Dependence on Neutralization. As a starting point, we assessed how neutralization influences the crystallinity and Young's modulus at room temperature. Young's modulus (E) was calculated from the slope of the uniaxial stress vs strain curve in the small-strain regime ($\epsilon < 5\%$). Weight fraction crystallinity was calculated by dividing the material's heat of fusion ΔH_f, obtained by differential scanning calorimetry (DSC), by 278 J/g for 100% crystalline polyethylene.[24] These weight fractions were converted to approximate crystalline volume fractions (ϕ_1) using representative density values of 1.00 and 0.94 g/cm^3 for the crystalline and amorphous regions, respectively.[25] Though the amorphous-phase density is expected to increase with MAA content and with neutralization,[25] the effects of such changes on the calculated values of ϕ_1 are no bigger than the uncertainty in the measurement of ΔH_f by DSC, as the endotherms are broad in these materials; the estimated uncertainty in ϕ_1 is ±0.01. Measurements were made on specimens stored at room temperature for a consistent 6 days after molding, as past studies[26−28] have found a significant dependence of E and ΔH_f on aging time, due to the slow formation of secondary crystals.

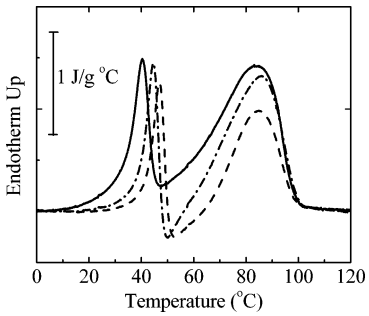

Figure 1. DSC heating thermograms of an E/MAA copolymer (22 wt % MAA) and two ionomers derived therefrom, all stored at room temperature for 6 days after molding: (—) 22-0Na, (– -) 22-26Na, and (– –) 22-48Na.

Table 1 presents the values of ϕ_1 and E at 25 °C for all materials studied. Neutralization reduces the primary crystal melting temperature (T_{m1}) only slightly, while the accompanying reduction in crystallinity (ϕ_1) is more notable, as reported in earlier work.[25,27,29] All of the DSC traces exhibited at lower-temperature endotherm near 45 °C (peak melting temperature T_{m2}), which results from the melting of secondary crystals which form during room temperature storage;[19,25] the prominence of this endotherm increases with MAA content. Figure 1 shows DSC traces for the 22 wt % E/MAA copolymer and two of its ionomer derivatives. Neutralization reduces the area of the primary endotherm and increases T_{m2}; ionic associations increase the local viscosity (effective segmental friction) of the material,[20,21] so that fewer ethylene sequences are able to crystallize during initial cooling, thus making more (and longer) ethylene sequences available for secondary crystallization.[19] In several materials of high ion content, such as the two ionomers in Figure 1, the DSC trace actually dips below the baseline between the primary and secondary endotherms, due to recrystallization of a portion of the ethylene sequences which were originally present in secondary crystals.[30]

While ϕ_1 decreases with neutralization, Table 1 shows that E simultaneously *increases*, though only modestly above 10−20% neutralization. This clearly indicates that the amorphous-phase modulus increases with neutralization, which evidently more than compensates for the reduction in ϕ_1 (a reduction in "hard phase" content, in the language of two-phase composites). In a previous study of unneutralized E/MAA copolymers, we found that high MAA contents produced high values of E, even though ϕ_1 was relatively low; this effect was traced to a rise in

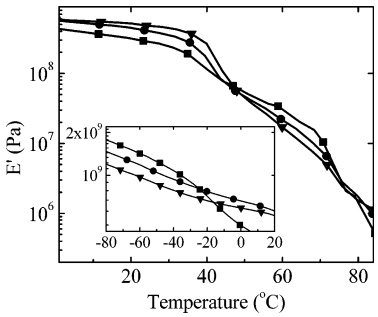

Figure 2. Storage modulus vs temperature for selected E/MAA ionomers with moderate ion contents (≈2 wt % Na^+), obtained from DMTA at 1 Hz: (■) 11.5-62Na, (●)15-51Na, (▲) 22-35Na. Inset shows the "B" transition region on an expanded scale.

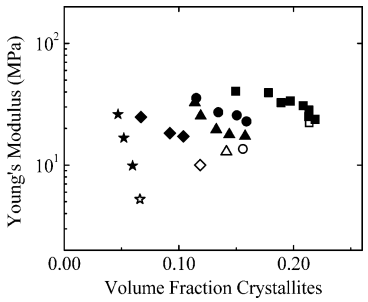

Figure 3. Young's modulus for all copolymers (open symbols) and ionomers at 60 °C plotted against volume fraction crystallinity: (■) 11.5%, (●) 15%, (▲) 19%, (◆) 22%, (★) 28 wt % MAA.

the amorphous-phase T_g through room temperature as the MAA content is increased.[22] For ionomers, physical cross-linking by the ionic associations should also influence the modulus. Separating and quantifying these various contributions to the modulus is the goal of the present paper.

The direct effect of ionic cross-linking is most evident when the materials are compared at temperatures well above the T_g of their parent E/MAA copolymers, where—in the simplest picture—the amorphous phase might be expected to consist of rubbery chains physically cross-linked through the ionic associations. The presence of two crystal populations, and differences in parent copolymer T_g (4−29 °C) at different MAA contents, makes the selection of a common comparison temperature a delicate task. Storage modulus (E') data for representative ionomers in Figure 2 show that the most suitable temperature is 60 °C, where the temperature dependence of E' is weakest; moreover, Table 1 shows that by 60 °C secondary crystal melting is complete, while primary crystal melting has scarcely begun. Unixaxial stress−strain testing was thus conducted at 60 °C; the E(60 °C) values are plotted in Figure 3 against ϕ_1, where ϕ_1 at 60 °C was estimated from the DSC trace, calculating ΔH_f between 60 °C and the final melting temperature.[22] At 60 °C, the expected trend of increasing E with increasing ϕ_1 is recovered, though there are still important differences between ionomers neutralized to different extents; comparison of the open symbols (E/MAA copolymers) and filled symbols (ionomers) in Figure 3 reveals that E(60 °C) increases with neutralization at constant ϕ_1, reflecting an increase in the amorphous-phase modulus.

To isolate and quantify the effect of ionic cross-linking on the amorphous-phase modulus, we employ the Davies model for two-phase composites:[31]

$$E_{comp}^{1/5} = \phi_1 E_1^{1/5} + \phi_2 E_2^{1/5} \quad (1)$$

In eq 1, E_{comp} is the Young's modulus for the semicrystalline

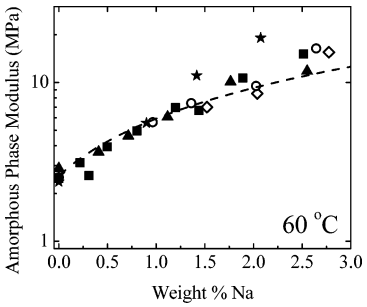

Figure 4. Amorphous phase modulus for all copolymers and ionomers at 60 °C, determined through the Davies equation, as a function of ion content: (■) 11.5%, (○) 15%, (▲) 19%, (◇) 22%, (★) 28 wt % MAA. Values for E/MAA copolymers are shown at 0% Na. Dashed curve is the modulus predicted by simple rubber elasticity theory.

ionomer, E_1 is the modulus for the polyethylene crystallites (taken[22] as 1450 MPa at 60 °C), E_2 is the amorphous phase modulus, and ϕ_1 and ϕ_2 are the volume fractions of crystallites and amorphous phase, respectively ($\phi_1 + \phi_2 = 1$). We have previously shown that the Davies model is a good quantitative descriptor for the Young's modulus of E/MAA copolymers;[22] by applying it here to the ionomers, we are considering the ionic aggregates to be part of an effectively homogeneous amorphous phase. Since the ionic aggregates in E/MAA ionomers are estimated to be of order 1 nm by SAXS,[7,12] while the primary crystallites are of order 10 nm thick (and of even larger lateral extent),[19] it is reasonable to mechanically coarse-grain the amorphous phase on the size scale of the primary crystallites.

Figure 4 plots the values of amorphous-phase modulus E_2 at 60 °C against ion content (wt % Na) in the materials; the latter is a measure of the ionic cross-link density. Indeed, taking this analogy further, if we assume that the ionic associations behave as long-lived cross-links on the time scale of the stress−strain measurement, we can compare these results with the prediction of ideal rubber elasticity theory, assuming high-functionality cross-links:[32]

$$E_2 = E_{ent} + 3\nu_i RT \quad (2)$$

where E_{ent} is the contribution due to chain entanglements, R is the gas constant, and ν_i is the density of elastically effective network strands defined by the ionic cross-links. If we take ν_i as equal to the number density of ionic groups (i.e., all ionic groups participate in ionic cross-links), then the dashed curve in Figure 4 is calculated, setting $E_{ent} = 2.6$ MPa from the average of the values determined for the E/MAA copolymers (no ions) and taking a representative density of 0.92 g/cm^3 at 60 °C. This highly idealized model describes the data for E_2-(60 °C) remarkably well, but we caution against overinterpretation, since as shown below, there is a significant rate dependence of the modulus for such materials in this temperature range. Indeed, one might ask how reasonable it is to approximate the ionic associations as long-lived cross-links, given that these same ionomers are melt-processable at higher temperatures.[4,20,21] In our previous work, we have estimated the average lifetime of an ionic association $\tau = 3$ ms for 11.5-61Na in the melt at 135 °C, with an activation energy of 80 kJ/mol.[21] A direct extrapolation yields $\tau = 0.6$ s at 60 °C, which is considerably shorter than the reciprocal of the Instron strain rate (0.038 s^{-1}). However, the presence of crystallites below T_{m1} might be expected to further restrict the motion of ionic groups relative to the melt; diffusion measurements of Van Alsten[33] show that this effect can further slow the motion of ionic groups at 60 °C by a factor of 40 over that predicted by a simple extrapolation

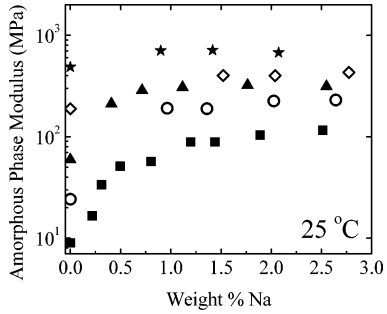

Figure 5. Amorphous phase modulus for all copolymers and ionomers at 25 °C, determined through the Davies equation, as a function of ion content: (■) 11.5%, (○) 15%, (▲) 19%, (◇) 22%, (★) 28 wt % MAA. Values for E/MAA copolymers are shown at 0% Na.

from the melt. Applying this factor of 40 makes the ionic association lifetime at 60 °C comparable to the reciprocal of the test rate employed, so the ionic associations may indeed be considered "long-lived" at 60 °C and below.

Figure 4 shows that the "direct" effect of ionic aggregation is to raise the modulus by a factor of up to ≈5× over that of the nonionic E/MAA copolymers. Yet inspection of Figure 2 shows that these materials have a modulus at room temperature higher by an order of magnitude than at 60 °C. Part of the modulus drop between 25 and 60 °C reflects the melting of secondary crystals, which decreases ϕ_1 typically by 0.02−0.06. To remove this effect, we employ eq 1 to calculate the amorphous-phase modulus E_2 at 25 °C (using[22] $E_1 = 3800$ MPa) and with ϕ_1 calculated from ΔH_f determined from 25 °C to the final melting temperature (encompassing the secondary crystals); values of E_2(25 °C) are plotted in Figure 5. It is immediately clear that at 25 °C E_2 is not at all a unique function of ionic content, unlike the behavior of E_2 at 60 °C shown in Figure 4; thus, it is clearly incorrect to attribute the increase in room temperature modulus on "ionomerization" to a simple, direct effect of ionic cross-linking. Inspection of the data at 0% Na (unneutralized E/MAA copolymers) shows a very strong increase in E_2(25 °C) with MAA content; as noted above and demonstrated in detail in our previous work,[22] this is a consequence of the amorphous-phase T_g rising through 25 °C as MAA content is increased over this range. The 28 wt % MAA copolymer already has[22] $T_g = 29$ °C before neutralization; thus, little increase in the room temperature modulus of this copolymer occurs upon neutralization (Figure 5 and Table 1). For the 11.5 wt % MAA copolymer, which has[22] $T_g = 4$ °C, a progressive increase in E_2(25 °C) with neutralization is observed, by up to an order of magnitude. But whether this increase results from the direct effect of ionic cross-linking as in Figure 4, or to an elevation of T_g upon neutralization, or to some combination of the two is unclear. Identifying the root cause of the behavior evident in Figure 5 requires a more detailed evaluation of the relaxation mechanisms present in these semicrystalline E/MAA ionomers, as discussed in the next section.

Phase Separation within the Amorphous Phase. Figure 6 shows E', E'' (loss modulus), and tan δ (loss tangent) curves as a function of temperature for 11.5% MAA ionomers at various neutralization levels. Several mechanical relaxations can be seen between −40 and +70 °C, where primary crystal melting starts to become significant. Similar relaxations have been observed in previous DMTA studies of E/(M)AA ionomers and have often been given various symbols and interpretations,[14−18] so to avoid confusion, we will simply label these relaxations as "A", "B", etc.

In Figure 6, the E/MAA copolymer and its lightly neutralized derivatives (<15% neutralized) exhibit only one clear relaxation

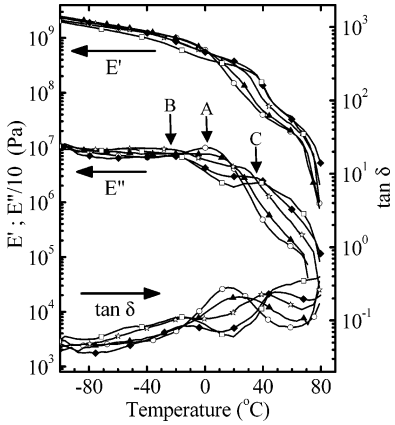

Figure 6. DMTA data (1 Hz) for selected 11.5 wt % MAA ionomers, all aged at room temperature for 6 days after molding: storage modulus (E'), loss modulus (E''), and loss tangent (tan δ): (○) 11.5-0Na, (▲)-11.5-10Na, (☆) 11.5-26Na, (◆)11.5-47Na, (□) 11.5-83Na. A, B, and C relaxations are indicated.

in the temperature region of interest, near 5 °C (E'' maximum), which we label "A"; this relaxation has been designated as β' or β in prior literature.[15,16,18] We have previously shown this relaxation to be the glass transition of the amorphous phase in these materials.[22] While polyethylene homopolymers often show an "α transition" characteristic of motion within the polyethylene crystals, E/MAA copolymers with 9 or more wt % MAA have such thin crystals that the α transition temperature is depressed, and no separate α-relaxation can be observed.[22,34] As the neutralization level is increased, the "A" relaxation splits into two:[14−18] one at lower temperature ("B") and one at higher temperature ("C"). All ionomers except 11.5-7Na and 11.5-10Na showed this split relaxation, which is consistent with the transition from A to B/C relaxations occurring at an ion (Na) content of 0.4 wt % (equivalent weight of 5800 g/equiv).

Though various explanations have been proposed for the origin of the B relaxation over the years, there now appears to be a consensus that this reflects the glass transition of ion-depleted domains within the amorphous phase,[16,18,35] consistent with the EHM model.[11] Page, Cable, and Moore reached a similar conclusion recently for semicrystalline tetrafluoroethylene-based (Nafion) ionomers.[36] In Figure 6, note that the B transition occurs at temperatures significantly lower than the T_g (A transition) in the acid copolymer; indeed, it is closer to the β relaxation temperature for low-density polyethylene homopolymer polymerized under similar conditions[22] ($T_\beta = -22$ °C). This implies that the amorphous regions responsible for the B relaxation have been largely depleted of MAA units, even when the neutralization level is rather low (as low as 16% neutralization for E/MAA 11.5). This curious result can be explained by the fact that unneutralized acid groups are known to preferentially associate with the ionic aggregates in Na^+-neutralized E/MAA ionomers.[20,37] This explanation is bolstered by comparison with literature data on Zn^{2+}-neutralized E/MAA[16] and E/AA[18] ionomers. Unneutralized acid groups do *not* preferentially associate with Zn^{2+} aggregates,[20,37] and indeed, when Zn^{2+} is the neutralizing cation, much higher neutralization levels are required to see the A relaxation split into B/C relaxations.[16] Moreover, the temperature of the B relaxation decreases steadily as full Zn^{2+}-neutralization is approached,[18] unlike the abrupt decrease in temperature which accompanies even partial Na^+-neutralization.

While the ion-poor regions are responsible for the B relaxation, devitrification of the ion-rich regions contributes to the C relaxation. However, observation and interpretation of

the C relaxation are complicated by the simultaneous melting of secondary crystals, and we defer its detailed consideration to the following section ("The C Relaxation"). For the present, the key point is that for all our materials showing the split B/C relaxation the B transition is below room temperature, while the C transition is above. Thus, the ion-poor regions—and only the ion-poor regions—are fully relaxed during a room temperature measurement of the modulus, which permits a clear interpretation of the unusual E_2(25 °C) behavior in Figure 5, as follows.

Consider first the ionomers derived from the 11.5 wt % MAA copolymer. At low neutralization levels (<0.4 wt % or <15% neutralization), E_2(25 °C) increases substantially, due both to ionic cross-linking and to the emergence of microphase separation within the amorphous phase. However, above 0.4 wt % Na (>15% neutralization), the amorphous phase modulus is essentially constant, since 0.4 wt % Na is already sufficient to sequester nearly all the MAA units within the ion-rich regions. Further neutralization may elevate the temperature of the C relaxation (ion-rich regions), but it does not substantially change the relative fractions of ion-rich and ion-poor material, so the room temperature modulus is scarcely affected when the ion content is increased beyond 0.4 wt %. However, increasing the MAA content in the copolymer *will* increase the fraction of the amorphous phase which is occupied by the ion-rich material, as nearly all of the MAA units are sequestered within these ion-rich regions. Thus, for materials with >0.4 wt % Na, there is a monotonic increase in E_2(25 °C) with MAA content (even though there is no substantial dependence on neutralization level).

That MAA content, and not neutralization level, determines the relative abundance of ion-rich and ion-poor regions can also be deduced from the DMTA data. The inset to Figure 2 shows the region of the B relaxation for three ionomers having ≈2 wt % Na but different MAA contents. For the 11.5 wt % MAA ionomer, a clear drop in E' by ~40% can be observed at T_B (−20 °C), while for the 15 and 22 wt % MAA ionomers, only weak inflections in the E' curves can be observed. These differences in the prominence of the B transition are a direct reflection of the larger volume fraction of ion-poor regions in the E/MAA 11.5 case, though the ion contents in all three materials are comparable.

The C Relaxation: Devitrification of Ion-Rich Regions and Melting of Secondary Crystals. Since the low-temperature B transition results from devitrification of ion-poor regions, it is natural to infer that the higher-temperature C transition reflects the devitrification of the corresponding ion-rich regions, consistent with the EHM model.[11] However, DSC shows that the secondary crystals also melt in this temperature range (35−50 °C; Figure 1 and Table 1), so the observed C relaxation may contain contributions from both processes. In this section, we take three distinct but complementary approaches to separating the amorphous and crystalline contributions to the DMTA C relaxation: (1) varying the test frequency, (2) allowing different lengths of time for secondary crystals to develop, and (3) changing the secondary crystal melting point through annealing.

Secondary crystal melting and amorphous phase devitrification can be resolved through variable-frequency DMTA,[16] since the latter process is frequency-dependent, while the former is not. Figure 7 shows DMTA data for ionomer 22-48Na acquired during a single heating run at three different frequencies, spaced roughly a decade apart; this material was chosen because it has the highest ion content among our ionomers. As the test frequency is raised or lowered, the location of the step drop in

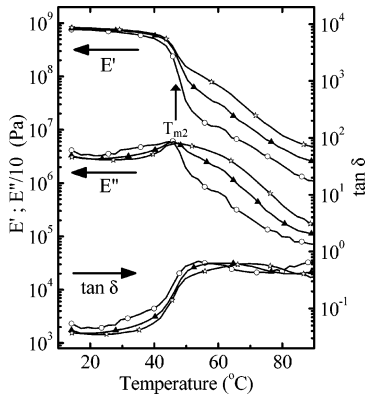

Figure 7. Frequency-dependent DMTA data for ionomer 22-48Na, aged at room temperature for 6 days after molding: storage modulus (E'), loss modulus (E''), and loss tangent (tan δ): (○) 0.16 Hz (1 rad/s), (▲) 1.6 Hz (10 rad/s), and (☆) 12.7 Hz (80 rad/s). Data were taken during a single heating ramp. The DSC-determined peak melting temperature for the secondary crystallites, T_{m2}, is indicated.

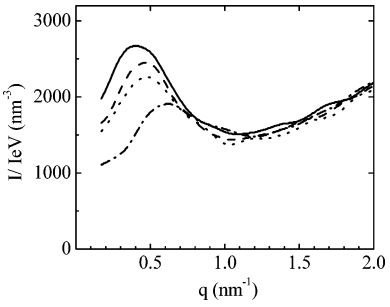

Figure 8. SAXS profiles of ionomer 15-67Na taken during the slow formation of secondary crystals at room temperature: (—) 0 h, (− −) 6 h, (- - -) 1 day, and (− -) 4 days after molding. Note progressive shift of peak to higher q as interlamellar secondary crystals form.

E' (47 °C) remains unchanged and identical to the melting point of the secondary crystals (T_{m2}). However, the magnitude of this step drop decreases steadily as the frequency is increased because the E' value above T_{m2} (at 55 °C, for example) increases progressively with frequency, by roughly 3× per decade. Such a strong frequency dependence is characteristic of a material in the vicinity of its glass transition. It is interesting to note that a somewhat attenuated frequency dependence (roughly 2×/decade) persists even at 90 °C, where nearly all the crystals have melted; this frequency dependence results from the finite lifetime of the ionic associations and concomitant relaxation of the polymer chains, as seen in melts of such ionomers.[21]

The contribution which secondary crystals make to the modulus can also be isolated, at least approximately, by measuring test specimens stored for various times at room temperature, since the secondary crystals develop over time scales of days. Figure 8 shows small-angle X-ray scattering (SAXS) patterns for specimens of ionomer 15-67Na taken after different periods of room-temperature storage. The peak near $q = 0.5$ nm^{-1}, which reflects the spacing between polyethylene crystallites, moves progressively to higher q with aging time as thin secondary crystals form between the primary crystals, thus reducing the average intercrystallite spacing.[19] Figure 9 shows DSC and DMTA results for similar aged specimens of 15-67Na. The sample tested as soon as practical after molding shows only a hint of a secondary crystal population by DSC, yet a significant (2×) drop in E' can be seen near 30 °C. We attribute this 2× reduction to the relaxation of the ion-rich amorphous regions.

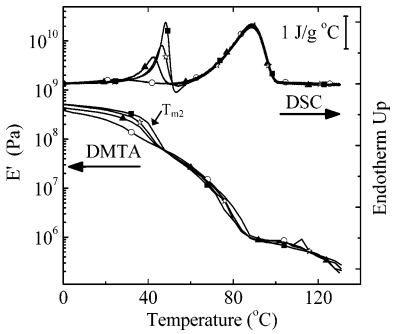

Figure 9. Parallel DSC (top) and DMTA (E', bottom; 1 Hz) data for specimens of ionomer 15-67Na, following periods of room temperature aging similar to those employed for SAXS in Figure 8: (○) 0 h, (▲) 6 h, (☆) 1 day, and (■) 6 days. Note step drop in E' as secondary crystals melt at T_{m2}.

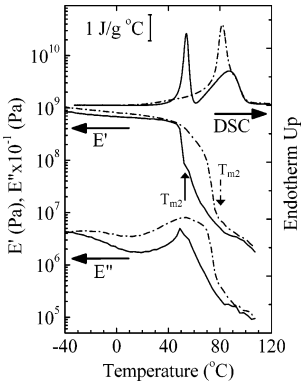

Figure 10. Parallel DSC (top) and DMTA (E', middle; E'', bottom; 1 Hz) data for specimens of ionomer 22-48Na with the following thermal histories: (—) aged at room temperature for 4 months; (— -) aged at room temperature for 4 months, followed by 2 h at 67 °C.

With increased aging time, Figure 9 shows that the secondary crystal endotherm increases in area and moves to slightly higher temperature, while the drop in E' increases in magnitude and also moves to slightly higher temperature;[27] after 4 days of annealing, the drop amounts to 5× in modulus. Note that once the secondary crystal melting is complete, the E' curves for the various thermal histories superimpose quite well; the larger modulus drop thus reflects an increase in E' on the low-temperature side of the transition. These secondary crystals contribute a maximum of 0.03 to ϕ_1 (6-day specimen), so a 5× modulus drop is far more than can be attributed to their melting, in the context of any isotropic two-phase composite model of which we are aware; the Davies model predicts a step of less than 1.2×. Indeed, even the product of these two factors—devitrification of the ion-rich regions (2×) and melting of the secondary crystals (1.2×)—is too small to explain the observed modulus drop. Thus, while two processes are operative in this temperature region, they are clearly not acting independently: the formation of secondary crystals synergistically raises the modulus of the amorphous phase, thus producing an unexpectedly large modulus drop when the secondary crystals melt.

Finally, the contributions from secondary crystal melting and amorphous phase devitrification can also be separated by changing the melting point of the secondary crystals (T_{m2}). This is easily accomplished by annealing the molded specimens at temperatures above room temperature; T_{m2} increases with annealing temperature, as longer sequences will crystallize preferentially at these higher temperatures and produce thicker secondary crystals.[30] Figure 10 shows DSC and DMTA results for specimens of 22-48Na annealed either at room temperature for 4 months or at 67 °C for 2 h. Though the overall melting enthalpies for the two specimens are quite similar when integrated from room temperature through final melting, the secondary crystals in the 67 °C-annealed sample now melt near 80 °C and indeed overlap in their melting range with the primary crystals. The E' curves for the two specimens are also quite different. In the 67 °C-annealed specimen, the devitrification of the ion-rich amorphous regions (relaxation C) can now be seen as a gradual drop in E' beginning near 50 °C (E'' maximum); the melting of the secondary (and primary) crystals produces the large drop in E' near 80 °C. Notably, the 67 °C-annealed specimen has a storage modulus at 60 °C which is 10× larger than that of the room temperature annealed specimen; this difference in E' is much larger than can be explained by the differences in ϕ_1 in this temperature range for the two thermal histories (0.09 vs 0.14), indicating that devitrification of the ion-rich amorphous regions is still far from complete in the 67 °C-annealed specimen.

Thus, for both the thermal histories employed in Figure 10, the melting of the secondary crystallites is accompanied by a reduction in the modulus of the amorphous phase; this reduction must reflect a relaxation of the ion-rich regions or a reduction in the topological continuity of the rigid portion of the amorphous phase, since the ion-poor amorphous regions have already relaxed at T_B (near −20 °C). The difference between the two cases is that in the 67 °C-annealed sample T_{m2} *exceeds* the temperature at which relaxation of the ion-rich regions (C) commences, while for the room temperature-annealed specimens, secondary crystal melting occurs first and is itself responsible for the reduction in continuity of the rigid portion of the amorphous phase.

Morphological Model for Synergy between Secondary Crystals and Ion-Rich Regions. Returning to the ideas of Eisenberg, Hird, and Moore,[11] the ion-rich regions can constitute a significant fraction of the amorphous phase even when the ion content is modest due to the immobilization of a layer of polymer adjacent to the aggregates. When the aggregates are small, as in styrene−methacrylate and ethylene−methacrylate ionomers, these "regions of restricted mobility" can overlap to produce a percolating rigid pathway through the amorphous regions. As the temperature is increased, one might expect a gradual "thinning" of these immobilized layers prior to complete devitrification, since these layers are dynamical constructs (rather than structural entities). Thinning of these layers would produce a progressive breakdown in the percolating pathways through the material and consequently a progressive reduction in the effective modulus of the amorphous phase prior to complete devitrification. This is certainly the case for styrene−methacrylate ionomers,[10] where the higher-temperature transition (C) is considerably broader than the low-temperature glass transition (B). Thus, for the 67 °C-annealed sample in Figure 10, the gradual E' decline between 50 and 70 °C reflects the breakdown of some of the percolating paths of rigid ion-rich regions in the amorphous phase; nonetheless, some of these paths remain even at 60 °C, and the amorphous phase still has a relatively high modulus (E_2' estimated as 170 MPa at 60 °C from eq 1). Note that these paths need only span the distance between crystallites[19] (≈20 nm) to produce a sample-spanning rigid pathway, since the crystals are themselves rigid entities. Once the crystals melt, however, no sample-spanning rigid paths remain, and E' drops to the low value (<5 MPa) characteristic of an E/MAA ionomer melt at this frequency.[21]

Consider now how thinner secondary crystals, as present in the room temperature-annealed specimen, would modify this behavior. These crystals necessarily form within the ion-poor

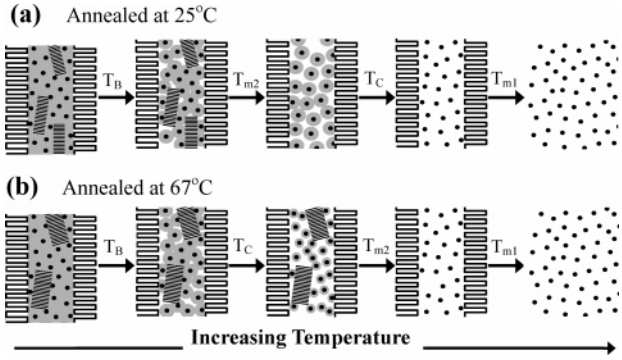

Figure 11. Schematic of morphological changes that E/MAA ionomers undergo upon heating, corresponding to the two thermal histories in Figure 10. Straight lines represent ethylene crystal stems; solid circles are ionic aggregates; gray and white shading denote vitrified and devitrified amorphous regions. Sample temperature increases from left to right. Top sequence represents a specimen wherein the secondary crystals formed at room temperature, while the bottom sequence represents a 67 °C-annealed specimen. In (a), secondary crystal melting at T_{m2} breaks the continuous hard (gray) paths through the amorphous phase, while in (b), these paths begin to break down prior to T_{m2} due to elevation of T_{m2} via annealing.

(ethylene-rich) regions, which are interspersed with the ion-rich regions. Thus, such secondary crystals can "connect" the ion-rich regions, forming percolating "hard" paths between the primary crystals, as the secondary crystals are also rigid entities. Yet when these secondary crystals melt, their absence will create breaks in the previously continuous rigid pathways between primary crystals, leading effectively to an amorphous phase with much lower modulus than below T_{m2}. This explains the large reductions in E and E' associated with the melting of these secondary crystals—reductions much larger than can be interpreted simply on the basis of reduced crystallinity, if the crystallites are considered to be the only "hard" entities in the system.

Figure 11 schematically represents these processes for E/MAA ionomers having the two thermal histories represented in Figure 10: (a) aged at room temperature and (b) annealed at 67 °C. At low temperatures, below T_B (near −20 °C), all amorphous segments are glassy, and the material has a correspondingly high modulus. At T_B, the ion-poor amorphous regions devitrify, and the modulus drops accordingly. The modulus drop at T_B is greater for materials with lower MAA content, but it is never large, because the ion-poor regions—broken up by both ion-rich regions and by crystallites—do not span the entire specimen.

As temperature is further increased, the next two events are devitrification of the ion-rich regions and melting of the secondary crystallites; which of these occurs first depends on the secondary crystallites' melting point and thus on the material's thermal history. The secondary crystals that form on room temperature aging (Figure 11a) melt at a low temperature ($T_{m2} \approx 45$ °C), and their melting breaks the percolated "hard" paths through the amorphous phase, leading to a large drop in the modulus. Annealing at 67 °C raises T_{m2} (to ≈80 °C), so that devitrification of the ion-rich regions commences prior to T_{m2}, but most of the modulus drop still does not occur until the onset of substantial crystal melting.

The key point here is that both the crystallites (especially the secondary crystallites) and the ion-rich regions *together* form sample-spanning paths which give rise to the modulus increases observed when E/MAA copolymers are "ionomerized" (neutralized). These paths can be broken, and the modulus greatly reduced, *either* when the crystallites melt or the restricted mobility zones surrounding the ionic aggregates cease to overlap. The relative order of these two events can be manipulated through specimen thermal history, leading to the very different linear mechanical responses shown in Figure 10, though the room temperature crystallinities and moduli of these two specimens are quite similar. Moreover, because the crystals participate in the percolating network, only a relatively small ion content is required to achieve a sample-spanning hard phase when compared with analogous amorphous ionomers (≈0.4 wt % Na^+ for E/MAA ionomers vs 1.2 wt % Na^+ for styrene/MAA ionomers[10]). Thus, the simultaneous presence of thin crystallites and ionic aggregates does more than complicate the morphology: synergy between the two yields a pronounced increase in material stiffness, while retaining sufficient "soft" material (the ion-poor regions) that typical E/MAA ionomers are quite tough even in impact testing.[28]

Conclusions

The results presented herein reveal the morphological origin of the modulus-temperature behavior in E/MAA ionomers, particularly the room temperature tensile modulus (E(25 °C)). Above a relatively low threshold ion content (0.4 wt % Na), the calorimetric and/or mechanical signatures of four distinct entities can be seen: primary crystallites, secondary crystallites, ion-poor regions, and ion-rich regions. The last of these four comprises the aggregated ionic groups, associated unneutralized MAA units, and immobilized layers of polymer surrounding the aggregates. Above the melting point of the primary crystals (T_{m1}), the material is an associating fluid. Below T_{m1}, the ionomer is effectively a composite of the rigid primary crystallites and a rubbery, ionically cross-linked amorphous phase; its modulus can be quantitatively described through the Davies equation. At room temperature, however, the secondary crystallites and the ion-rich regions together form continuous "hard" paths through the amorphous phase, leading to anomalously high values of both the amorphous phase modulus (E_2(25 °C)) and the composite modulus (E(25 °C)). The ion-poor regions devitrify below room temperature (at T_B), but do not form sample-spanning pathways, so their relaxation is not accompanied by a large modulus decrease. However, melting of the secondary crystals at T_{m2} disrupts the continuity of the "hard" paths through the amorphous phase and produces a large modulus decrease. Annealing the specimen at elevated temperatures thickens the secondary crystals and raises T_{m2}, so that the onset of devitrification of the ion-rich regions (at T_C) precedes T_{m2}, but the bulk of the relaxation (and modulus drop) still accompanies the secondary crystal melting. The ability to tune T_{m2} through annealing permits the modulus at moderately elevated temperatures (60 °C) to be tuned over an order-of-magnitude range through thermal history, without affecting the room temperature modulus or degree of crystallinity. These findings represent an essential starting point for a broader understanding of structure−property relationships in semicrystalline ionomers.

Acknowledgment. This work was generously supported by DuPont Packaging and Industrial Polymers, Sabine River Works. The authors acknowledge invaluable assistance and stimulating discussions with John Paul, Steven Pesek, George Prejean, Brian Roach, and David Walsh of DuPont. We thank Stephanie Lopina and Pierre Vanhoorne for the preparation of several of the 11.5 wt % MAA ionomers.

References and Notes

(1) Eisenberg, A.; Kim, J.-S. *Introduction to Ionomers*; Wiley: New York, 1998.

(2) Schlick, S., Ed. *Ionomers: Characterization, Theory, and Applications*; CRC Press: Boca Raton, FL, 1996.
(3) Tant, M. R., Mauritz, K. A., Wilkes, G. L., Eds. *Ionomers: Synthesis, Structure, Properties and Applications*; Blackie Academic & Professional: London, 1997.
(4) Longworth, R. In *Ionic Polymers*; Holliday, L., Ed.; John Wiley & Sons: New York, 1975.
(5) Longworth, R.; Vaughan, D. J. *Nature (London)* **1968**, *218*, 85.
(6) Register, R. A.; Cooper, S. L. *Macromolecules* **1990**, *23*, 318.
(7) Quiram, D. J.; Register, R. A.; Ryan, A. J. *Macromolecules* **1998**, *31*, 1432.
(8) Hird, B.; Eisenberg, A. *J. Polym. Sci., Polym. Phys.* **1990**, *28*, 1665.
(9) Kim, J.-S.; Wu, G.; Eisenberg, A. *Macromolecules* **1994**, *27*, 814.
(10) Kim, J.-S.; Jackman, R. J.; Eisenberg, A. *Macromolecules* **1994**, *27*, 2789.
(11) Eisenberg, A.; Hird, B.; Moore, R. B. *Macromolecules* **1990**, *23*, 4098.
(12) Yarusso, D. J.; Cooper, S. L. *Polymer* **1985**, *26*, 371.
(13) Hird, B.; Eisenberg, A. *Macromolecules* **1992**, *25*, 6466.
(14) Rees, R. W.; Vaughan, D. J. *Polym. Prepr. (Am. Chem. Soc., Div. Polym. Chem.)* **1965**, *6*, 287.
(15) MacKnight, W. J.; McKenna, L. W.; Read, B. E. *J. Appl. Phys.* **1967**, *38*, 4208.
(16) Tachino, H.; Hara, H.; Hirasawa, E.; Kutsumizu, S.; Tadano, K.; Yano, S. *Macromolecules* **1993**, *26*, 752.
(17) Otocka, E. P.; Kwei, T. K. *Macromolecules* **1968**, *1*, 401; **1969**, *2*, 110.
(18) Khanna, Y. P.; Wenner, W. M.; Krutzel, L. *Macromolecules* **1988**, *21*, 268.
(19) Loo, Y. L.; Wakabayashi, K.; Huang, Y. E.; Register, R. A.; Hsiao, B. S. *Polymer* **2005**, *46*, 5118.
(20) Vanhoorne, P.; Register, R. A. *Macromolecules* **1996**, *29*, 598.
(21) Tierney, N. K.; Register, R. A. *Macromolecules* **2002**, *35*, 6284.
(22) Wakabayashi, K.; Register, R. A. *Polymer* **2005**, *46*, 8838.
(23) Register, R. A.; Bell, T. R. *J. Polym. Sci., Polym. Phys.* **1992**, *30*, 569.
(24) Wunderlich, B. *Macromolecular Physics*; Academic Press: New York, 1973.
(25) Marx, C. L.; Cooper, S. L. *J. Macromol. Sci., Phys.* **1974**, *B9*, 19.
(26) Kohzaki, M.; Tsujita, Y.; Takizawa, A.; Kinoshita, T. *J. Appl. Polym. Sci.* **1987**, *33*, 2393.
(27) Hirasawa, E.; Yamamoto, Y.; Tadano, K.; Yano, S. *Macromolecules* **1989**, *22*, 2776.
(28) Akimoto, H.; Kanazawa, T.; Yamada, M.; Matsuda, S.; Shonaike, G. O.; Murakami, A. *J. Appl. Polym.* Sci. **2001**, *81*, 1712.
(29) Wilson, F. C.; Longworth, R.; Vaughan, D. J. *Polym. Prepr. (Am. Chem. Soc., Div. Polym. Chem.)* **1968**, *9*, 505.
(30) Tsujita, Y.; Shibayama, K.; Takizawa, A.; Kinoshita, T.; Uematsu, I. *J. Appl. Polym. Sci.* **1987**, *33*, 1307.
(31) Davies, W. E. A. *J. Phys. D* **1971**, *4*, 1176.
(32) Graessley, W. W. *Polymeric Liquids & Networks: Structure and Properties*; Garland Science: New York, 2004.
(33) Van Alsten, J. G. *Macromolecules* **1996**, *29*, 2163.
(34) Popli, R.; Glotin, M.; Mandelkern, L.; Benson, R. S.*J. Polym. Sci., Polym. Phys. Ed.* **1984**, *22*, 407.
(35) MacKnight, W. J.; Earnest, T. R., Jr. *J. Polym. Sci., Macromol. Rev.* **1981**, *16*, 41.
(36) Page, K. A.; Cable, K. M.; Moore, R. B. *Macromolecules* **2005**, *38*, 6472.
(37) Han, K.; Williams, H. L. *J. Appl. Polym. Sci.* **1991**, *42*, 1845.

MA052081V